

## COMPARISON OF INFORMATION ON SLEEP APNOEA CONTAINED IN TWO SYMMETRIC EEG RECORDINGS

Monika A. Prucnal, Adam G. Polak

Wrocław University of Science and Technology, Faculty of Electronics, B. Prusa 53/55, 50-317 Wrocław, Poland  
(✉ [monika.a.prucnal@pwr.edu.pl](mailto:monika.a.prucnal@pwr.edu.pl), +48 71 320 6247, [adam.polak@pwr.edu.pl](mailto:adam.polak@pwr.edu.pl))

### Abstract

*Electroencephalogram* (EEG) is one of biomedical signals measured during all-night polysomnography to diagnose sleep disorders, including sleep apnoea. Usually two central EEG channels (C3-A2 and C4-A1) are recorded, but typically only one of them are used. The purpose of this work was to compare discriminative features characterizing normal breathing, as well as obstructive and central sleep apnoeas derived from these central EEG channels. The same methodology of feature extraction and selection was applied separately for the both synchronous signals. The features were extracted by combined discrete wavelet and Hilbert transforms. Afterwards, the statistical indexes were calculated and the features were selected using the analysis of variance and multivariate regression. According to the obtained results, there is a partial difference in information contained in the EEG signals carried by C3-A2 and C4-A1 EEG channels, so data from the both channels should be preferably used together for automatic sleep apnoea detection and differentiation.

Keywords: sleep apnoea detection, EEG signal, discrete wavelet transforms, Hilbert transforms, analysis of variance, multivariate regression analysis.

© 2019 Polish Academy of Sciences. All rights reserved

## 1. Introduction

*Polysomnography* (PSG) is a conventional method for assessment of sleep disorders, in particular sleep apnoea, basing on biosignals recorded in sleep laboratories [1–3]. Its primary effect is the evaluation of incidence of breathing disturbances and the overall quality of sleep. *Electroencephalogram* (EEG) is one of biomedical signals registered during all-night PSG [1], representing the electrical activity of the brain and revealing changes in functioning of the central neural system. In sleep studies, EEG is usually used to detect sleep stages related to *waking up* (W) and two main phases: REM (*rapid eye movement*) and NREM (*non-rapid eye movement*) [4, 5].

The basic approach to the analysis of EEG signal, especially when detecting sleep disorders, is the analysis of brainwaves classified as: delta (0.5–4 Hz), theta (4–8 Hz), alpha (8–14 Hz), beta (14–30 Hz) and gamma (30–80 Hz) [6]. Apart from these main five brainwaves, there are also other waveforms, as saw-tooth waves, sleep spindles and K complexes [6].

Sleep apnoea is one of the most common sleep disorders affecting about 4% of adult men and 2% of adult women [1]. It is characterized by the repeated and temporary cessation of airflow for at least 10 seconds or its reduction (hypopnea, characterised by a more than 50% decrease in airflow and associated decrease in blood oxygen saturation) [1]. These breathing events cause fragmentation of sleep, affecting health and well-being of patients. There are three types of apnoea: *central* (CSA), *obstructive* (OSA) and *mixed one* (MSA) [1]. The most common of them is OSA, characterized by repetitive episodes of upper airway obstruction, while maintaining the respiratory rhythm. CSA is seen as the complete elimination or reduction of ventilation effort. Its direct cause is usually a failure in the central nervous system influencing the work of cerebral hemispheres or brainstem. In MSA, both the central and obstructive factors are the sources of apnoea episodes. Such apnoea episodes affect the EEG signal, changing the brainwaves. Specifically, they decrease the amplitude of signal before and during an episode, increasing, however, the energy of alpha and beta waves, with arousals appearing after them [7–13], and these changes have a regional character [14].

The brainwaves are recorded from the central and occipital areas of the scalp during PSG [15, 16]. Standard electrode leads are based on the International 10/20 System of Electrode Placement, including C3-A2 or C4-A1 and O1-A2 or O2-A1 channels [16], which make it possible to clearly capture necessary EEG waveforms [15]. The central placements (C3-A2 and C4-A1) are used to distinguish characteristic sleep stage attributes, including vertex sharp waves, K complexes, sleep spindles and delta waves [16]. A review of methods for digital EEG signal analysis in obstructive sleep apnoea, the so-called *quantitative EEG* (qEEG), has been published recently [17].

Although both central channels C3-A2 and C4-A1 are typically recorded during PSG [18], the data from only one channel were usually used in previous approaches to the automatic apnoea detection [2, 19–22]. On the other hand, some studies revealed asymmetries in activity of the human brain's hemispheres during sleep, and thus differences in the content of symmetrical EEG channels [23–26]. In particular, such inter-hemispheric asynchrony was observed during OSA [27, 28]. Nevertheless, a relatively little attention has been devoted to this phenomenon, and, according to the best knowledge of the authors, such differences have not been studied in the context of automatic sleep apnoea detection. Therefore, the question arises whether it is sufficient to use one, freely chosen from two EEG channels (C3-A2 or C4-A1), or whether it would be more reasonable to use both of them for the automatic detection of sleep apnoea.

The aim of this research was to compare the features characterising normal breathing (NB), OSA and CSA, derived from two symmetric EEG channels in the central areas of the scalp (C3-A2 and C4-A1). The identity or diversity of such features can answer the question about the usefulness of data obtained from one or two EEG channels in the algorithms detecting sleep apnoea epochs. To this end, the same feature extraction and selection methods were applied separately to both EEG channel recordings. The used here methodology of finding the best discriminative features within the three classes (NB, OSA and CSA) was proposed recently [29]: first the features characterising EEG epochs were extracted using the combined discrete wavelet and Hilbert transforms and descriptive statistical methods, then the feature selection was performed applying the analysis of variance and multivariate regression analysis, and finally the resulting feature vectors obtained from two channels were compared.

## 2. Materials and methods

The underlying methodology was described in more detail elsewhere [29] and will be presented briefly below. It is shown in Fig. 1. All procedures of data processing were written in MATLAB R2017b (The MathWorks, USA).

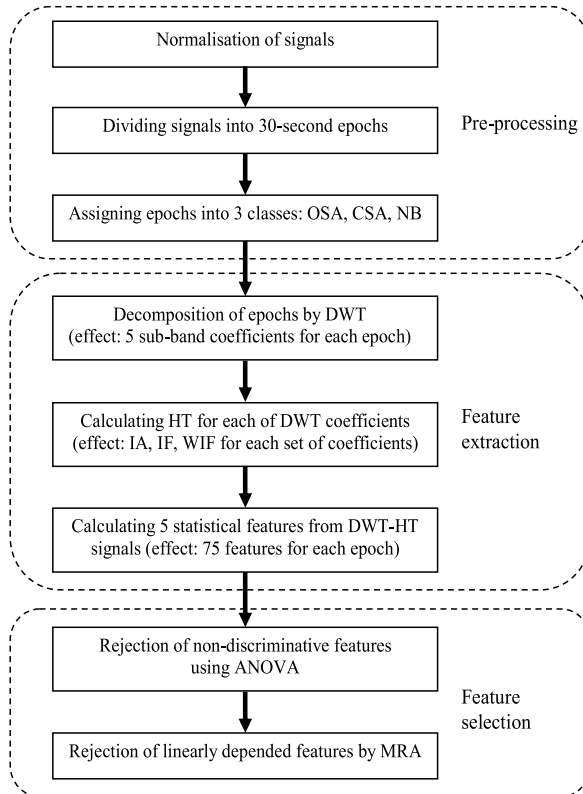


Fig. 1. A diagram of EEG signal processing.

### 2.1. EEG data

The data from the *PhysioBank* database were used in this research [18]. They contain, among others, the whole-night EEG signals from two symmetric channels (C3-A2 and C4-A1) sampled at 128 Hz from 25 patients (4 women and 21 men). The respiratory events were scored and classified into obstructive, central and mixed apnoea and hypopnea events with a resolution of 1 s. [18]. First, all of the overnight signals were normalised within a range  $\langle -1, 1 \rangle$  to eliminate inter-subject differences. Then, the 30-second epochs [1, 2, 5, 11, 22, 27, 29, 30] were extracted from the signals around the well-defined respiratory events of apnoea or hypopnea. Lastly, the prepared database was divided into three balanced classes: NB, OSA, and CSA (see Fig. 2).

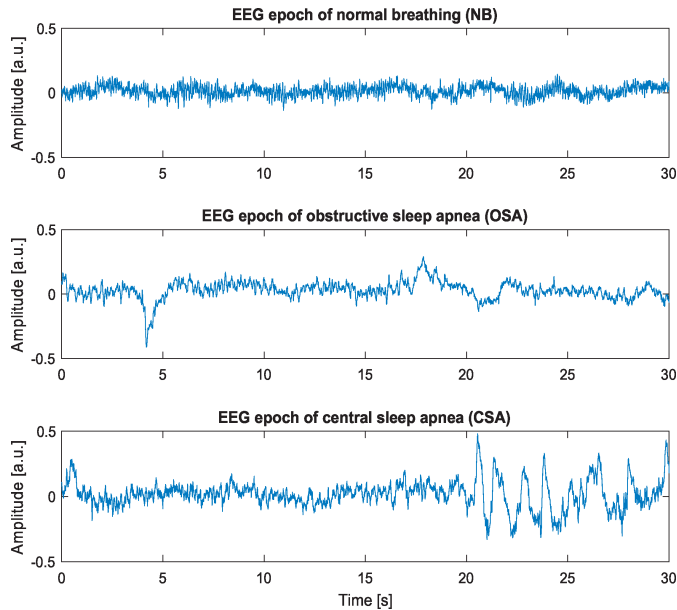


Fig. 2. Examples of EEG epochs for normal breathing, and obstructive and central sleep apnoea.

## 2.2. Feature extraction

The extraction of features from the synchronised EEG epochs was performed for the C3-A2 and C4-A1 channels using the combined *discrete wavelet transform* (DWT) and *Hilbert transform* (HT). Such an approach enables to decompose the signals into the brainwave frequency ranges (DWT) and then to calculate their instantaneous attributes as amplitude, frequency and amplitude-weighted frequency (HT) [29].

DWT is a time–frequency signal analysis method returning approximation ( $a$ ) and detailed ( $d$ ) coefficients at a given level [31]. Finally, a signal  $x$  is decomposed into a weighted sum of  $J$ -level series of wavelet functions  $\psi$  and a scaling function  $\varphi$  (covering all wavelets of higher levels):

$$x(n) = \sum_{j=1}^J \sum_k d_{j,k} \psi_{j,k}(n) + \sum_k a_{J,k} \varphi_{J,k}(n). \quad (1)$$

The sets of detailed  $D_j = \{d_{j,k}\}$  and approximation coefficients  $A_J = \{a_{J,k}\}$  were used to extract features from  $x$ . In this work, the Daubechies wavelets of order 3 were chosen, often used to decompose the EEG signal because of their similarity to its characteristic waves and spikes [5, 32, 33]. The number of final sub-bands depends on the maximal number of selected levels of decomposition. Taking into account the sampling frequency (128 Hz) and the frequency ranges of brainwaves, 4 levels of decomposition were used, resulting in the following sub-band coefficients:  $D_1$  (32–64 Hz),  $D_2$  (16–32 Hz),  $D_3$  (8–16 Hz),  $D_4$  (4–8 Hz) and  $A_4$  (0–4 Hz), corresponding to the brainwaves: gamma, beta, alpha, theta and delta, respectively. An example of the 4th level DWT decomposition of an EEG epoch representing OSA is shown in Fig. 3.

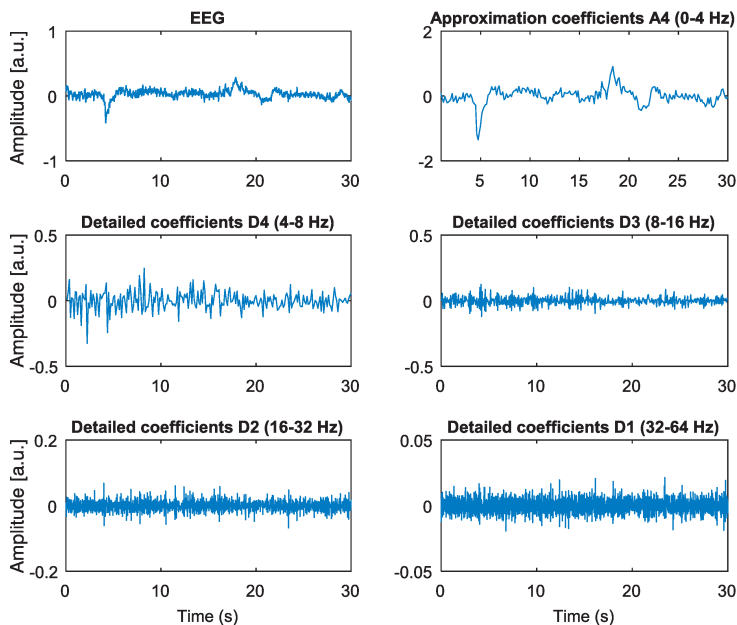


Fig. 3. Approximation and detailed coefficients from DWT of an EEG epoch representing OSA.

HT returns an analytic signal  $Y$  from a real data sequence  $y$ , which is expressed as:

$$Y(t) = y(t) + jh(t) = A(t)e^{j\phi t}, \quad (2)$$

where  $h$  is an HT of  $y$ ;  $A$  is an instantaneous amplitude and  $\phi$  is an instantaneous phase of  $Y$ . The analytic signal can be further used to calculate *instantaneous amplitudes* (IA) and *frequencies* (IF) [34]. An instantaneous frequency ( $f$ ) is the derivative of  $\phi$ :

$$f(t) = \frac{1}{2\pi} \frac{d\phi}{dt}. \quad (3)$$

The attributes IA and IF were computed for each of the above DWT coefficients, and then the samples corresponding to negative instantaneous frequencies or lying outside the frequency ranges related to a given DWT level were excluded [29, 35]. Additionally, an *amplitude-weighted instantaneous frequency* (WIF) was calculated as [29]:

$$f_w(t) = \frac{A(t)}{\frac{1}{N} \sum_{t=1}^N A(t)} f(t), \quad (4)$$

where  $N$  is the number of samples. WIF is used to better represent the frequencies of dominant energy [29]. The instantaneous amplitude, frequency and amplitude-weighted frequency (only the samples corresponding to non-negative IF lying in the range of 8–16 Hz) yielded by the HT of the 3rd level detailed coefficients ( $D_3$ ) from the EEG epoch representing OSA (see Fig. 3) are presented in Fig. 4.

The last step of feature extraction was the calculation of five statistical indexes (mean, standard deviation, skewness, kurtosis and median) for the 15 signals characterising each of EEG epochs.

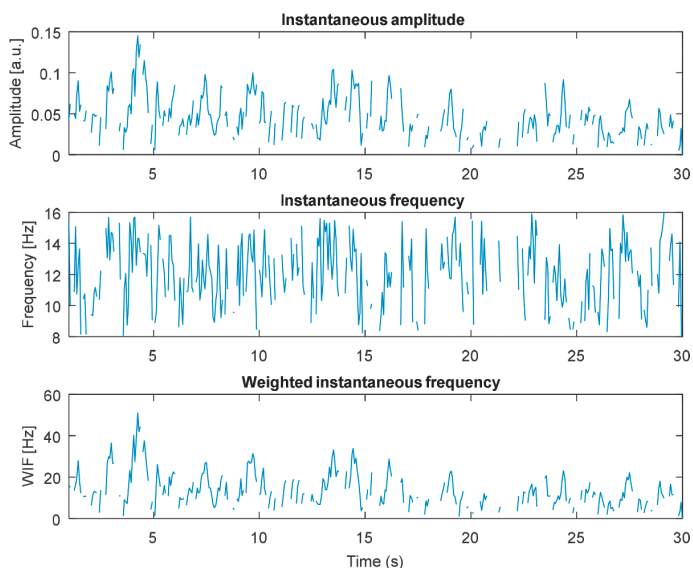


Fig. 4. Instantaneous amplitude, frequency and weighted frequency yielded by HT of  $D_3$  shown in Fig. 3.

### 2.3. Feature selection

Choosing adequate methods for the selection of features is a complex task. One of approaches is using *filters* that select variables by ranking them, *e.g.* in terms of correlation coefficients. Chosen in such a way, the most relevant features are usually suboptimal. However, this method is faster than *wrapper* or *embedded* ones and the outcome is independent from a final classifier (not used in this work) [36].

The result of feature selection by a suboptimal method depends often on the feature sequence. To include this fact in the subsequent analyses, the order of features was set randomly 30 times and the next steps were repeated also 30 times using these feature permutations.

The feature selection was performed using the *one-way analysis of variance* (ANOVA) and *multivariate regression analysis* (MRA). ANOVA was used to check whether the examined set included discriminative features and the weakly differentiating ones were finally rejected ( $p < 0.05$ ). Next, MRA was carried out, enabling the backward elimination of features that were almost linearly dependent on others according to the adjusted coefficient of determination ( $\bar{R}^2 > 0.97$ ).

## 3. Results

The final balanced database used in this work amounted to 3750 synchronised epochs for each of EEG channels (C3-A2 and C4-A1), with 1250 elements (randomly selected from sometimes bigger sets) belonging to the three classes (NB, OSA and CSA). The feature extraction procedures returned vectors with originally 75 elements characterising each of the EEG epochs. The feature selection was repeated 30 times for different permutations of extracted features (however with the same order for the two channels) and the obtained *feature vectors* (FVs) from C3-A2 and C4-A1 channels were compared.

The selected features differed for the two channels in all of the 30 analysed cases. The FVs were reduced from 75 to 44–51 for C3-A2 and to 43–50 features for C4-A1 channel, respectively.

The amount of selected features associated with the brainwaves is shown in Table 1 separately for the two channels. The independent two-sample *t*-tests for equal sample size were used to compare the mean values of these features in two EEG channels. Before that, the equality of variances was checked in each instance (two-sample *F*-test), and statistically unequal variances were found for the delta, alpha and beta brainwaves – this information was further used during the *t*-tests. First, the two-tailed *t*-tests were performed, and the equality of means could not be rejected for gamma brainwaves. Then, the one-tailed *t*-tests were performed for the rest of sub-bands to test the alternative hypothesis that the number of C3-A2 discriminative features is either greater or smaller than that from the C4-A1 channel. The results are presented in Table 1. This analysis has indicated that the numbers of features selected from the C4-A1 channel’s delta and theta waves are significantly greater than those selected from channel C3-A2, while the numbers of features selected from the C3-A2 channel’s alpha and beta waves are significantly greater than those selected from channel C4-A1.

Table 1. Numbers of features selected from C3-A2 and C4-A1 channels representing the brainwaves (\* statistically significant difference).

Brainwaves	Numbers of features (mean ± SD)		
	C3-A2	C4-A1	<i>p</i> -value
delta (A4)*	8.60 ± 0.56	10.20 ± 1.19	2.26 · 10 <sup>-8</sup>
theta (D4)*	10.63 ± 0.56	12.60 ± 0.62	6.42 · 10 <sup>-19</sup>
alpha (D3)*	9.90 ± 1.06	8.00 ± 0.00	5.20 · 10 <sup>-11</sup>
beta (D2)*	10.03 ± 0.61	8.63 ± 0.96	9.3 · 10 <sup>-9</sup>
gamma (D1)	8.37 ± 0.96	8.43 ± 0.97	0.79

Additionally, all the features were analysed in terms of their discriminative power in respect of both channels. The four following cases were considered (with the threshold value of 15 counts per 30 repetitions of feature selection): 1) a given feature was selected for both channels; 2) it was selected only for C3A2 but not for C4-A1 channel; 3) it was selected only for C4A1 but not for C3A2 channel; and 4) it was rejected for both channels. As a result, 41 mutual features were selected for both EEG channels. The numbers of features were similar for each of the brainwaves (7 for delta, 10 for theta and 8 for alpha, beta and gamma). A more interesting outcome, however, concerns the features selected separately for only one channel. These features, four for C3-A2 and seven for C4-A1 channel, are presented in Tables 2 and 3, respectively.

Table 2. Features characterising separately channel C3-A2.

No.	EEG channel C3-A2		
	Brainwave	Signal from HT	Statistical index
1	alpha (D3)	IA	kurtosis
2	alpha (D3)	WIF	standard deviation
3	beta (D2)	WIF	standard deviation
4	gamma (D1)	IA	skewness

Table 3. Features characterising separately channel C4-A1.

No.	EEG channel C4-A1		
	Brainwave	Signal from HT	Statistical index
1	delta (A4)	IA	median
2	delta (A4)	WIF	skewness
3	delta (A4)	WIF	kurtosis
4	theta (D4)	IF	standard deviation
5	theta (D4)	IA	standard deviation
6	theta (D4)	WIF	standard deviation
7	gamma (D1)	WIF	kurtosis

#### 4. Discussion

The results demonstrate the difference between right (C4-A1) and left (C3-A2) EEG recordings from the central region of the scalp during all-night sleep with episodes of sleep apnoea. These differences are noticeable especially in the features of delta, theta, alpha and beta waves. In total, there are 48 discriminative features retrieved from the right hemisphere (C4-A1) and 45 features coming from the left hemisphere (C3A2). This suggests a slightly more dynamic behaviour of the right hemisphere during sleep in apnoeic subjects. This activity concerns mainly the delta and theta waves (0.5–4 and 4–8 Hz, respectively), having more features in C4-A1 channel. On the contrary, the features from the alpha and beta waves (8–14 and 14–30 Hz, respectively) dominate in C3-A2 channel.

Most of discriminative features were extracted from the D4 (theta wave) coefficients of DWT (13 features), showing the importance of low-frequency EEG components in apnoea detection. However, for the other coefficients of DWT, their amounts were also significant and almost equal (10 features for A4, D3 and D1, and 9 features for D2). In addition, the features were mostly related to all of the HT instantaneous attributes: frequency (18 features), amplitude (17 features) and amplitude-weighted frequency (17 features) – a result emphasising the usefulness of the recently proposed approach to feature extraction [29]. Finally, the most frequently selected statistical indexes (13, 12 and 11 features, respectively) were standard deviation, kurtosis and median.

Summarising the above findings, the difference in FVs extracted from two symmetrical, central EEG channels was observed. Nevertheless, this result does not directly imply the differences in interhemispheric connectivity or synchronization. It is also possible that the observed dissimilarities result from the operation of reference electrodes (A1 and A2). Measuring (or recalculating) these signals against a common reference would clarify this issue, however it is impossible when using the retrospective data from the PhysioNet. Although the features do not enable to draw conclusions about the pathophysiological background, it has been shown that they enable the automatic detection and differentiation of sleep apnoea [29]. Moreover, it is worth stressing that there are studies showing the asymmetry in functioning of the hemispheres during sleep, including sleep apnoea [14]. A significantly greater amount of the delta waves in the right frontal and central regions during sleep than in those of the left one, and no differences for other brain regions, were observed [25]. Another work, investigating hemispheric asymmetries during sleep in relation to the sleep stages, showed that the alpha waves dominated in the left hemisphere in all channels during NREM sleep, whereas the dominance of the theta waves was observed in the right hemisphere during NREM sleep and in the left hemisphere during REM sleep in

the central-parietal regions [24]. Moreover, the apnoea-hypopnoea events are strongly correlated with NREM stages [30]. Additionally, other authors found the right hemisphere night-time superiority and the left hemisphere daytime superiority [26], as well as temporary changes in the hemispheric dominance during sleep related to the state of airways (open or closed, as in OSA) [27, 28]. According to the former research, the delta waves dominated in the left hemisphere and beta waves dominated in the right hemisphere during undisturbed airflow through the airways, and there were no noticeable differences between the hemispheres during apnoea episodes [28]. In contrast, the latter paper suggested that the functional asymmetries of brain regions during sleep apnoea occurred and were associated with EEG arousals [27]. The results of this work are generally in line with the previous findings summarised above.

## 5. Conclusion

The comparison of features characterising NB, OSA and CSA, derived from two symmetric EEG channels in the central areas of scalp (left C3-A2 and right C4-A1), showed that some discriminative features belonged separately to only one of the channels. For the C3-A2 channel these features were in the alpha and beta frequency ranges, while for the C4-A1 channel they were in the delta and theta ranges. Most of these features are standard deviation, kurtosis and median derived from the analysis of the instantaneous frequency, amplitude or amplitude-weighted frequency of DWT coefficient describing the frequency range of the theta (D4) waves.

The main finding of this work is that there is a partial difference in information contained in the EEG signals derived from two symmetric EEG channels C3-A2 and C4-A1, and that the data from the both channels should be used together for automatic sleep apnoea detection and differentiation. The above results enable to undertake next steps towards the clinical application of qEEG to the detection and differentiation of sleep apnoea.

## References

- [1] Anonymous. (2001). *International classification of sleep disorders, revised: Diagnostic and coding manual*. Chicago, IL: American Academy of Sleep Medicine.
- [2] Zhou, J., Wu, X.M., Zeng, W.J. (2015). Automatic detection of sleep apnea based on EEG detrended fluctuation analysis and support vector machine. *Journal of Clinical Monitoring and Computing*, 29(6), 767–772.
- [3] Nitkiewicz, S., Barański, R., Kukwa, A., Zając, A. (2018). Respiratory disorders – measuring method and equipment. *Metrol. Meas. Syst.*, 25(1), 187–202.
- [4] Kleitman, N., Asernisky, E. (1953). Regularly occurring periods of eye motility, and concomitant phenomena, during sleep. *Science*, 118(3062), 273–274.
- [5] Prucnal, M., Polak, A.G. (2017). Effect of feature extraction on automatic sleep stage classification by the artificial neural network. *Metrol. Meas. Syst.*, 24(2), 229–240.
- [6] Chokroverty, S., Thomas, R., Bhatt, M. (2014). *Atlas of Sleep Medicine*. Philadelphia: Elsevier Saunders.
- [7] Walsleben, J.A., O'Malley, E.B., Bonnet, K., Norman, R.G., Rapoport, D.M. (1993). The utility of topographic EEG mapping in obstructive sleep apnea syndrome. *Sleep*, 16(8), S76–S78.
- [8] Bandla, H., Gozal, D. (2000). Dynamic changes in EEG spectra during obstructive apnea in children. *Pediatric pulmonology*, 29, 359–365.

- [9] Dingli, K., Assimakopoulos, T., Fietze, I., Witt, C., Wraith, P.K., Douglas, N.J. (2002). Electroencephalographic spectral analysis: detection of cortical activity changes in sleep apnoea patients. *European Respiratory Journal*, 20, 1246–1253.
- [10] Halász, P., Terzano, M., Parrino, L., Bódizs, R. (2004). The nature of arousal in sleep. *Journal of Sleep Research*, 13(1), 1–23.
- [11] Coito, A.L., Sanches, J. (2011). Assessment of Obstructive Sleep Apnea Syndrome by spectral analysis of physiological parameters. *1st Portuguese Meeting in Bioengineering*, IEEE, Lisbon, 1–6.
- [12] Eckert, D.J., Younes, M.K. (2014). Arousal from sleep: implications for obstructive sleep apnea pathogenesis and treatment. *Journal of Applied Physiology*, 116(3), 302–313.
- [13] Cohen, M.X. (2014). *Analyzing neural time series data: theory and practice*. Massachusetts, MIT Press.
- [14] Jones, S.G., Riedner, B.A., Smith, R.F., Ferrarelli, F., Tononi, G., Davidson, R.J., Benca, R.M. (2014). Regional reductions in sleep electroencephalography power in obstructive sleep apnea: a high-density EEG study. *Sleep*, 37(2), 399–407.
- [15] Luecken, L.J., Gallo, L.C. (2008). *Handbook of Physiological Research Methods in Health Psychology*. Los Angeles: SAGE Publications.
- [16] Mattice, C., Brooks, R., Lee-Chiong, T. (2012). *Fundamentals of Sleep Technology*. Philadelphia: Lippincott Williams & Wilkins.
- [17] Puskás, S., Kozák, N., Sulina, D., Csiba, L., Magyar, M.T. (2017). Quantitative EEG in obstructive sleep apnea syndrome: a review of the literature. *Reviews in the Neurosciences*, 28(3), 265–270.
- [18] Goldberger, A.L., Amaral, L.A.N., Glass, L., Hausdorff, J.M., Ivanov, P.Ch., Mark, R.G., Mietus, J.E., Moody, G.B., Peng, C.K., Stanley, H.E. (2000). PhysioBank, PhysioToolkit, and PhysioNet: Components of a New Research Resource for Complex Physiologic Signals. *Circulation*, 101(23), 215–220.
- [19] Gosavi, P.B., Singh, R. (2017). Automatic sleep apnea detection based on entropy of multi-band EEG signal mechanism. *7th International Conference on Recent Trends in Engineering, Science and Management*, Pune, 728–735.
- [20] Sezgin, N., Tagluk, M.E. (2009). Energy based feature extraction for classification of sleep apnea syndrome. *Computers in Biology and Medicine*, 39(11), 1043–1050.
- [21] Tagluk, M.E., Sezgin, N. (2011). A new approach for estimation of obstructive sleep apnea syndrome. *Expert Systems with Applications*, 38(5), 5346–5351.
- [22] Shahnaz, C., Minhaz, A.T., Ahamed, S.T. (2016). Sub-frame based apnea detection exploiting delta band power ratio extracted from EEG signals. *IEEE Region 10 Conference (TENCON)*, Marina Bay Sands, 190–193.
- [23] Pereda, E., Gamundi, A., Nicolau, M.C., Rial, R., González, J. (1999). Interhemispheric differences in awake and sleep human EEG: a comparison between non-linear and spectral measures. *Neuroscience Letters*, 263(1), 37–40.
- [24] Roth, C., Achermann, P., Borbely A.A. (1999). Frequency and state specific hemispheric asymmetries in the human sleep EEG. *Neuroscience letters*, 271(3), 139–142.
- [25] Sekimoto, M., Kato, M., Kajimura, N., Watanabe, T., Takahashi, K., Okuma, T. (2000). Asymmetric interhemispheric delta waves during all-night sleep in humans. *Clinical Neurophysiology*, 111(5), 924–928.
- [26] Casagrande, M., Bertini, M. (2007). Night-time right hemisphere superiority and daytime left hemisphere superiority: A reprogramming of laterality across wake-sleep-wake states. *Biological psychology*, 77(3), 337–342.

- [27] Swarnkar, V., Abeyratne, U.R. (2006). Statistical analysis of EEG arousals in sleep apnea syndrome. *Proc. 24th IASTED International Conference on Biomedical Engineering (BioMED 2006)*, Innsbruck, 282–287.
- [28] Rial, R., Gonzalez, J., Gene, L., Akaarir, M., Esteban, S., Gamundi, A., Barcelo, P., Nicolau, C. (2013). Asymmetric sleep in apneic human patients. *American Journal of Physiology-Regulatory, Integrative and Comparative Physiology*, 304(3), 232–237.
- [29] Prucnal, M.A., Polak, A.G. (2018). Analysis of features extracted from EEG epochs by discrete wavelet decomposition and Hilbert transform for sleep apnea detection. *Proc. 40th Annual International Conference of the IEEE EMBC 2018*, Honolulu, 287–290.
- [30] Jung, D.W., Hwang, S.H., Lee, Y.J., Jeong, D.U., Park, K.S. (2016). Apnea–hypopnea index estimation using quantitative analysis of sleep macrostructure. *Physiological Measurement*, 37(4), 554–563.
- [31] Sundararajan, D. (2015). *Discrete Wavelet Transform: A Signal Processing Approach*. Singapore: Wiley.
- [32] Lin, R., Lee, R.G., Tseng, C.L., Zhou, H.K., Chao, C.F., Jiang, J.A. (2006). A new approach for identifying sleep apnea syndrome using wavelet transform and neural networks. *Biomedical Engineering: Applications, Basis and Communications*, 18(3), 138–143.
- [33] Gandhi, T., Panigrahi, B.K., Anand, S. (2011). A comparative study of wavelet families for EEG signal classification. *Neurocomputing*, 74(17), 3051–3057.
- [34] Poularikas, A.D. (1999). *Formulas and Tables for Signal Processing*. Boca Raton: CRC Press LLC.
- [35] Hsu, M.-K., Sheu, J.-C., Hsue, C. (2011). Overcoming the negative frequencies – instantaneous frequency and amplitude estimation using osculating circle method. *Journal of Marine Science and Technology*, 19(5), 514–521.
- [36] Guyon, I., Elisseeff, A. (2003). An introduction to variable and feature selection. *Journal of Machine Learning Research*, 3(3), 1157–1182.